Hindawi
Advances in Condensed Matter Physics
Volume 2018, Article ID 5018460, 10 pages
https://doi.org/10.1155/2018/5018460

Research Article

Influence of Blood Vessels on Temperature during High-Intensity Focused Ultrasound Hyperthermia Based on the Thermal Wave Model of Bioheat Transfer

Qiaolai Tan,[1,2] **Xiao Zou**,[1] **Hu Dong**,[1] **Yajun Ding**,[3] **and Xinmin Zhao**[1]

[1]*School of Physics and Electronics, Hunan Normal University, Changsha 410081, China*
[2]*School of Electronic Information and Electrical Engineering, Xiangnan University, Chenzhou 423000, China*
[3]*College of Information Science and Engineering, Hunan Normal University, Changsha 410081, China*

Correspondence should be addressed to Xiao Zou; shawner@hunnu.edu.cn

Received 15 June 2018; Accepted 8 August 2018; Published 6 September 2018

Academic Editor: Shuqing Chen

The coupled effects of blood vessels and thermal relaxation time on temperature and thermal lesion region in biological tissue during high-intensity focused ultrasound (HIFU) hyperthermia are numerically investigated. Considering the non-Fourier behavior of heat conduction in biological tissue, the traditional Pennes bioheat equation was modified to thermal wave model of bioheat transfer (TWMBT). Consequently, a joint physical model, which combines TWMBT for tissue and energy transport equation for blood vessel, is presented to predict the evolution of temperature and the thermal lesion region. In this study, pulsatile blood flow is first introduced into numerical study of HIFU hyperthermia, and thermal relaxation time, ultrasonic focus location, blood vessel radius, and blood flow velocity are all taken into account. The results show that the thermal relaxation time plays a key role in the temperature and the thermal lesion region. Larger thermal relaxation time results in lower temperature and smaller thermal lesion region, which indicates that TWMBT leads to lower temperature and smaller thermal lesion region compared to Pennes bioheat transfer model. In addition, we found that the ultrasonic focus location and blood vessel radius significantly affected the temperature and thermal lesion region, while the heartbeat frequency and amplitude factor of pulsating blood flow as well as the average velocity of blood flow had only a slight effect.

1. Introduction

High-intensity focused ultrasound (HIFU) is a promising noninvasive technology, which can rapidly produce a local high temperature of more than 70°C in target tissues for the purpose of thermal ablation [1, 2]. In 1942, Lynn [3] designed a focused ultrasound generator to produce focal heating to destruct the focal area deep in the fresh liver tissue without damage to the intervening tissue. Thereafter, HIFU technology had been paid more and more attention by scientists and doctors, especially since the rapid development of ultrasonic imaging technology in 1990s [4]. HIFU hyperthermia had been used to ablate solid tumors, including soft tissue sarcomas and cancers of the prostate, liver, kidney, breast, and pancreas [5]. The accurate thermal dose at the lesion location plays a decisive role in the clinical success of HIFU hyperthermia. Accordingly, it is necessary to study the temperature and the thermal dose of lesion region [6, 7].

In general, the temperature of biological tissue was predicted by Pennes bioheat transfer model because of its simplicity and practicability. It is well known that the model was built on the classical Fourier's law, implying an infinite thermal propagation velocity and an instantaneous thermal effect [8, 9]. That is to say, any heat perturbation in the biological tissue can be reached anywhere at the same time, which had aroused controversy among many scientists. To overcome this physically unreasonable drawback, Cattaneo and Vernotte independently proposed a generalized non-Fourier law heat conduction equation by introducing a lagging time called "relaxation time" [10, 11]. In addition, the non-Fourier behavior of heat conduction in non-homogenous medium requiring a relaxation time had been experimentally verified

by several researchers [12–14]. The reasonable relaxation time was in the range of 0.464-6.825s according to the convective heat transfer coefficient and the available properties of blood and tissue in Zhang's research [15]. In addition, TWMBT had many applications. For example, Dai studied skin burn injury subjected to radiation heating [16]. Jaunich analyzed the temperature distributions in the skin tissue medium during short pulse laser irradiation [17]. However, to our knowledge, few studies have been done on HIFU hyperthermia employing TWMBT until now, especially considering biological tissue with blood vessel.

Recently, Jiang employed HIFU to ablate tumors near significant blood vessels clinically [18]. In addition, several numerical studies of the effects of blood vessels on temperature and thermal lesion region in ultrasound hyperthermia had attracted the interests of many researchers. Pennes treated the blood vessel and bone mathematically exactly as the soft tissue and presumed that the blood and surrounding tissue were completely thermal equilibration [19]. This approach is valid for tissue with capillaries. Nevertheless, several researches implied that the thermal equilibration between the large blood vessels (diameters larger than 0.2 mm) and surrounding tissues was broken [20–22], and the large vessels in biological tissue should be considered. For instance, Kolios [20] examined the effects of blood flow on the thermal lesion dimensions and temperature distribution during focused ultrasound surgery. The blood vessel was coaxial with acoustic axis, and the ultrasonic focus was located in the center of the blood vessel. Hariharan [21] presented a three-dimensional physical model to investigate the efficacy of high-intensity focused ultrasound procedures targeted near large blood vessel, which was located outside the 6 dB width of the beam. Solovchuk [22] put forward an acoustic-thermal-fluid coupling model to study the influence of blood vessel on temperature, taking the effect of acoustic streaming into account. However, the temperature field computation was based on Pennes bioheat transfer model in most previous studies, neglecting the non-Fourier effects on thermal transfer, and the quantitative effects of the blood vessel on temperature and thermal lesion region in the heated tissue are still ambiguous. In our work, the effects of blood vessels on temperature and thermal lesion region based on TWMBT during HIFU hyperthermia will be comprehensively investigated, including various factors associated with blood vessels. In addition, pulsatile blood flow generated by the periodic pumping of heart contraction will be taken into consideration, which is firstly introduced into numerical study of HIFU hyperthermia. We believe that this study is significant for HIFU hyperthermia.

2. Theory

The HIFU transducer is a spherical cap with an aperture radius a of 35 mm, a focal length R of 62.64 mm, and a center frequency f of 1 MHz, and the transducer and biology tissue are placed in the water. The geometric configuration of physical model is shown in Figure 1.

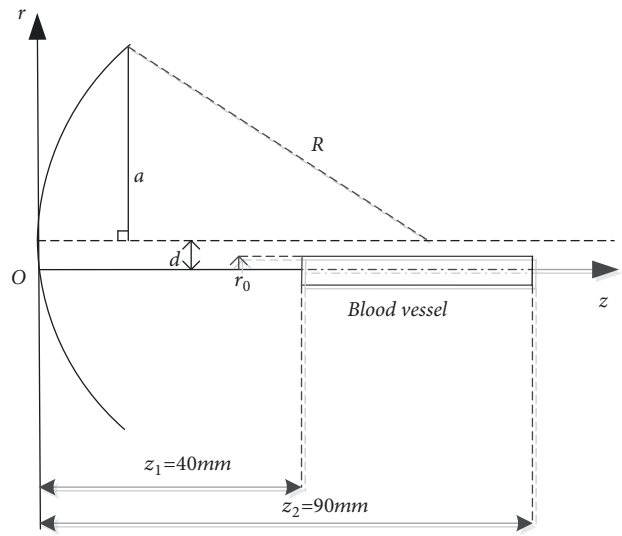

Figure 1: Geometric configuration of physical model. The tissue containing a large blood vessel, a cylinder with radius of 35 mm and length of 50 mm, is placed at $z_1 = 40\,mm$. The blood vessel is at the center of the tissue, r_0 is the radius of the blood vessel, and d is the distance between ultrasonic focus and central axis of blood vessel. The computational domain Ω is $-35\,mm \le r \le 35\,mm$ and $0 \le z \le 90\,mm$, abbreviated as $r, z \in \Omega$.

2.1. Acoustic Model for Ultrasound Wave Propagation. To model the ultrasound wave propagation in thermoviscous medium incorporating the effects of absorption, diffraction, and nonlinearity, a widely used Westervelt equation was employed, which can be written as follows [23]:

$$\left(\nabla^2 - \frac{1}{c_0^2}\frac{\partial^2}{\partial t^2}\right)p + \frac{\delta}{c_0^4}\frac{\partial^3 p}{\partial t^3} + \frac{\beta}{\rho c_0^4}\frac{\partial^2 p^2}{\partial t^2} = 0 \tag{1}$$

where ∇^2, p, c_0, t are Laplace operator, acoustic pressure, ultrasonic velocity, and time, respectively; $\beta = 1 + (B/2A)$ is the nonlinearity coefficient; and $\delta = 2\alpha c_0^3/\omega^2$ is the acoustic diffusivity accounting for thermoviscous effect in the fluid, where ω is the acoustic angular frequency and α is the acoustic absorption coefficient. The values of acoustic parameters used in this study are listed in Table 1 [24].

2.2. Thermal Energy Model for Tissue Heating. The heat conduction based on the classic Fourier is as follows:

$$q\left(\vec{r}, t\right) = -k\nabla T\left(\vec{r}, t\right) \tag{2}$$

where q denotes heat flux; K, $\vec{r}$, and ∇T the thermal conductivity, position vector, and temperature gradient, respectively; minus denotes that the direction of heat transfer is opposite to the temperature gradient. Generally, the bioheat transfer equation can be shown below:

$$\rho_t C_t \frac{\partial T}{\partial t} = -\nabla q - W_b C_b\left(T - T_a\right) + Q_{ext} \tag{3}$$

Table 1: Values of acoustic parameters in this study.

Material	$\rho/Kg\,m^{-3}$	$c_0/m\,s^{-1}$	$\alpha/Np\,m^{-1}\,MHz^{-1}$	β
Water	998	1524	0.025	5.0
Tissue	1060	1584	9.0	7.0
Blood	1060	1584	1.5	7.0

Table 2: Values of thermal parameters in this study.

Material	$K/W\,m^{-1}\,^{\circ}C^{-1}$	$C/J\,Kg^{-1}\,^{\circ}C^{-1}$	$W_b/Kg\,m^{-3}\,s^{-1}$
Water	0.6	4180	0
Tissue	0.5	3700	0.5
Blood	0.5	3840	0

Combining formula (2) with (3), a famous Pennes bioheat transfer equation can be obtained [19]:

$$\rho_t C_t \frac{\partial T}{\partial t} = K\nabla^2 T - W_b C_b \left(T - T_a\right) + Q_{ext} \tag{4}$$

where C_t and ρ_t are the specific heat and density of tissue, respectively; C_b, W_b, and T_a are the specific heat, perfusion rate, and initial temperature of blood, respectively; and all the values of thermal parameters in this study are listed in Table 2 [24]. Q_{ext} is the ultrasound heat deposition source term which can be calculated by employing time-averaged over one acoustic period by numerical integration [25]:

$$Q_{ext} = \frac{2\delta}{\rho c_0^4} \left\langle \left(\frac{\partial p}{\partial t} \right)^2 \right\rangle \tag{5}$$

It is well known that the heat conduction in the Pennes bioheat transfer equation is based on Fourier law. To incorporate the non-Fourier behavior, Cattaneo and Vernott proposed a modified heat conduction equation as follows [10, 11]:

$$q\left(\vec{r}, t\right) + \tau \frac{\partial q\left(\vec{r}, t\right)}{\partial t} = -K\nabla T\left(\vec{r}, t\right) \tag{6}$$

where τ is thermal relaxation time, which denotes a time lag between heat flux and temperature gradient, leading to significant non-Fourier thermal behavior. Based on (3) and (6), TWMBT can be expressed as follows [26]:

$$\begin{aligned} \rho_t C_t \left(\frac{\partial T}{\partial t} + \tau \frac{\partial^2 T}{\partial t^2} \right) &= K\nabla^2 T - W_b C_b \left(T - T_a\right) + Q_{ext} \\ &\quad + \tau \left(-W_b C_b \frac{\partial T}{\partial t} + \frac{\partial Q_{ext}}{\partial t} \right) \end{aligned} \tag{7}$$

In this paper, the physical model discussed in the next is the perfused tissue containing a large blood vessel. To compute the temperature field, the physical model should be split into two regions, one is the tissue region with perfusion [20], and the other is the blood region with a large blood vessel.

In the region without large blood vessel, TWMBT is used to compute the temperature field in the perfused tissue region. In the region with a large blood vessel resulting in the local cooling, an advective term $-\rho_b C_b u(r)(\partial T/\partial z)$ is added in the heat diffusion equation. The energy transport equation is as follows [20]:

$$\rho_b C_b \frac{\partial T}{\partial t} = K\nabla^2 T - \rho_b C_b u\left(r, t\right) \frac{\partial T}{\partial z} + Q_{ext} \tag{8}$$

In this study, the pulsatile blood flow in the blood vessel is considered, with the hypothesis that the blood vessel is rigid and the blood flow is laminar, incompressible, and Newtonian fluid. The pulsatile blood flow resulting from the periodic pumping of heart contraction is divided into a steady part and an oscillatory one [27]:

$$u\left(r, t\right) = u_s\left(r\right) + u_\phi\left(r, t\right) \tag{9}$$

$$u_s\left(r\right) = 2u_{ave}\left(1 - \frac{r^2}{r_0^2}\right) \tag{10}$$

$$\begin{aligned} &u_\phi\left(r, t\right) \\ &= \frac{8\mu\left(fac\right)u_{ave}}{\rho_b \omega_p r_0^2} \mathrm{Re}\left\{ \left[\frac{J_0\left(\eta\left(r/r_0\right)i^{3/2}\right)}{J_0\left(\eta i^{3/2}\right)} - 1 \right] e^{i\omega_p t} \right\} \end{aligned} \tag{11}$$

where $u(r, t)$ is the velocity of pulsatile blood flow. $u_s(r)$ is steady parabolic velocity of blood flow, which is relation to the corresponding Poiseuille flow velocity in steady blood flow; $u_\phi(r, t)$ represents the oscillatory velocity of blood flow in the rigid blood vessel; u_{ave} is the average velocity of blood flow; μ is dynamic viscosity of blood; $\eta = r_0/\sqrt{\mu/\rho_b\omega_p}$ is the Womersley number; fac characterizes the relative intensity of the pulsatile flow; ω_p is the angular frequency of heartbeat; $f_p = \omega_p/2\pi$ denotes the heartbeat frequency varied from 1 to 3Hz [28]; and J_0 is zero-order Bessel function of the first kind.

To evaluate the performance of the HIFU treatment, thermal dose is usually used to estimate the tissue damage. The thermal dose depends on the final time t_f and temperature level T, which is developed by Sapareto and Dewey [29]:

$$t_{43} = \int_0^{t_f} R^{(T-43)} dt \approx \sum_0^{t_f} R^{(T-43)} \Delta t \tag{12}$$

where t_{43} is the thermal dose equivalent time at 43°C. $R = 2$ if $T \geq 43^{\circ}C$ and $R = 4$ if $37^{\circ}C < T < 43^{\circ}C$. The threshold value

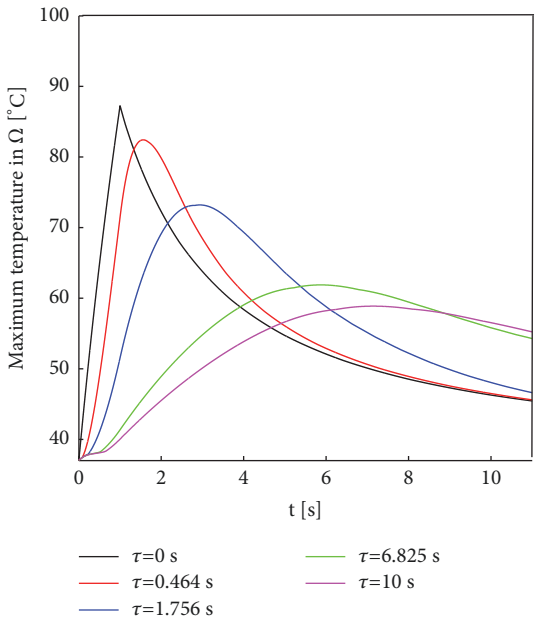

FIGURE 2: Maximum temperature in space $r, z \in \Omega$ versus time with different thermal relaxation time for $p_0 = 1.5 \times 10^5\ pa$, $r_0 = 1\ mm$, $d = 1.5\ mm$, $u_{ave} = 5\ cm/s$, $f_p = 1\ Hz$, $fac = 0.5$, $t_h = 1\ s$.

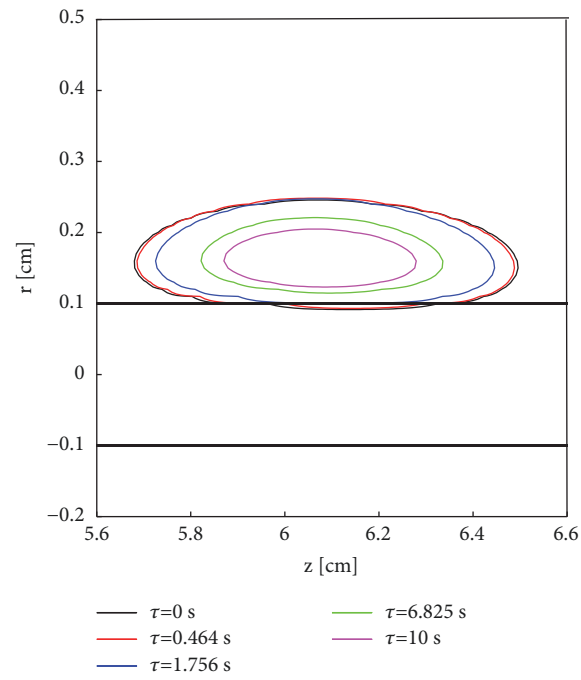

FIGURE 3: Thermal lesion region in space $r, z \in \Omega$ with different thermal relaxation time for $p_0 = 1.5{\times}10^5\ pa, r_0 = 1\ mm, d = 1.5\ mm$, $u_{ave} = 5\ cm/s$, $f_p = 1\ Hz$, $fac = 0.5$, $t_h = 1\ s$.

of an isothermal dose value of 240 *min* at 43°C was usually selected to predict the size of the thermal lesion region [30].

The initial condition is

$$T_t(r, z, 0) = T_b(r, z, 0) = T_a = 37^\circ\mathrm{C} \tag{13}$$

where T_t, T_b are temperature of tissue and blood flow, respectively. At the interface Γ between the tissue and blood vessel, the continuity condition of temperature is imposed.

$$T_t(r, z, t) = T_b(r, z, t) \quad \text{at } \Gamma \tag{14}$$

In this manuscript, (1), (7), and (8) are calculated on a polar cylindrical grid using the explicit finite-difference time-domain (FDTD) method as described in [31]. The spatial grids for the simulation are $\Delta z = \Delta r = 10^{-4}\ m$. The time step for acoustic field and temperature field simulation are $10^{-8}\ s$ and $10^{-4}\ s$, respectively [31].

3. Results and Discussions

3.1. Thermal Relaxation Time. Here, the influences of thermal relaxation time τ on hyperthermia treatment are investigated. To simplify the physical problem, we neglected the boiling cavitations. The ultrasonic transducer is excited by sinusoidal wave and the amplitude of acoustic pressure p_0 at the surface of the transducer is $1.5 \times 10^5\ pa$, the ultrasound heating time t_h is 1 *s*, and the thermal relaxation time τ is set to 0, 0.464, 1.756, 6.825, 10 *s* [15]. The heartbeat frequency f_p is set to 1Hz [28], and amplitude factor *fac* is 0.5. When $\tau = 0$, the thermal wave model of bioheat transfer becomes Pennes bioheat transfer model.

Figure 2 shows the time variation of the maximum temperature under different thermal relaxation time. The peak temperatures in space $r, z \in \Omega$ are 87.258°C, 82.432°C, 73.209°C, 61.88°C, 58.872°C at time 1*s*, 1.565 *s*, 2.939 *s*, 5.87 *s*, 7.147 *s* for $\tau = 0$, 0.464, 1.756, 6.825, 10 *s*, respectively. The greater the thermal relaxation time, the lower the peak temperature in biological tissue, and the greater the delay time reaching to the peak temperature. Besides, the peak temperature decreases immediately when the ultrasound power source is turned off at time $t = 1\ s$ for $\tau = 0$, but continues to increase for $\tau \neq 0$ (e.g., $\tau = 0.464, 1.756, 6.825, 10\ s$). This phenomenon is mainly due to infinite thermal propagation speed in biological tissue when $\tau = 0$ and finite thermal propagation speed when $\tau \neq 0$. The finite thermal propagation speed means that the thermal energy needs a certain amount of time to spread within the biological tissue, which is the physical significance of the thermal relaxation time. Meanwhile, a larger thermal relaxation time results in a larger delay time because of smaller thermal propagation speed in biological tissue.

In Figure 3, we present the thermal lesion region in space $r, z \in \Omega$ with different thermal relaxation time. The thermal lesion is an elliptical shape with the size $0.82\ cm \times 0.16\ cm$, $0.8\ cm \times 0.16\ cm$, $0.72\ cm \times 0.15\ cm$, $0.52\ cm \times 0.11\ cm$, $0.41\ cm \times 0.08\ cm$ for $\tau = 0$, 0.464, 1.756, 6.825, 10 *s*, respectively. There is only tiny difference to lesion size between $\tau = 0$ and $\tau = 0.464\ s$, but the lesion size decreases from $0.82\ cm \times 0.16\ cm$ to $0.41\ cm \times 0.08\ cm$ when thermal relaxation time varies from 0 to 10 *s*, which is almost reduced 75%. This can be easily understood that the peak temperature is 87.258°C for $\tau = 0$ and 58.872°C for $\tau = 10\ s$ from Figure 2. Consequently, it can be concluded that TWMBT results in lower temperature and smaller thermal lesion

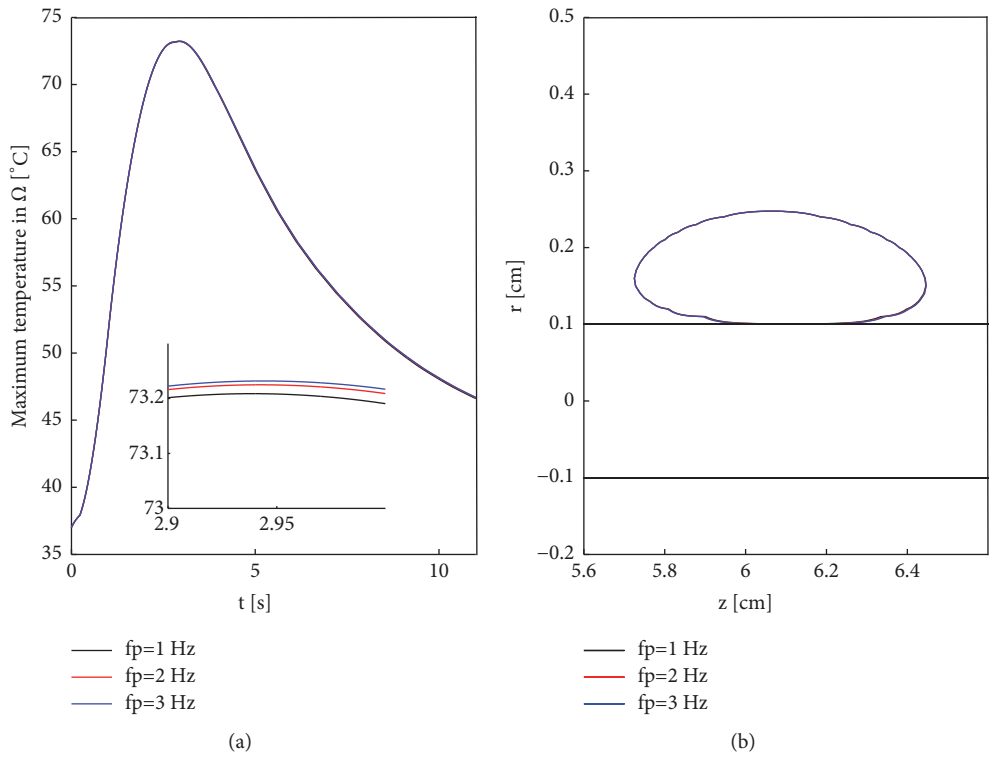

FIGURE 4: Effect of heartbeat frequency f_p on HIFU hyperthermia: (a) maximum temperature in space $r, z \in \Omega$ versus time; (b) thermal lesion region. Here, $p_0 = 1.5 \times 10^5\ pa$, $r_0 = 1\ mm$, $d = 1.5\ mm$, $u_{ave} = 5\ cm/s$, $fac = 0.5$, $t_h = 1\ s$.

region compared to the classical Pennes bioheat transfer model.

3.2. Pulsatile Blood Flow. Figure 4 shows effect of heartbeat frequency f_p on maximum temperature-time change and thermal lesion region. Figure 5 shows the effects of amplitude factor fac and different blood flow velocity forms (steady parabolic velocity $u_s(r)$ and pulsatile velocity $u(r,t)$) on maximum temperature-time change, respectively. There is almost no difference in maximum temperature evolution and thermal lesion region for different heartbeat frequencies in Figure 4. Subgraphs of maximum temperature variations in the time range from 2.9 s to 3.0 s are shown in Figures 4(a) and 5, respectively. Noteworthily, the largest difference in peak temperature is only about 0.02°C, indicating that heartbeat frequency f_p and amplitude factor fac almost have no difference on maximum temperature evolution and thermal lesion region. Meanwhile, although there is oscillatory velocity $u_\phi(r,t)$ in pulsatile blood flow, the steady parabolic velocity $u_s(r)$ can still be instead of time-dependent pulsatile velocity $u(r,t)$ for simplicity.

3.3. The Distance between Ultrasonic Focus and Central Axis of Blood Vessel. In Figure 6, the simulated maximum temperature versus time is presented with different distance between ultrasonic focus and central axis of blood vessel. The peak temperature is 47.85°C when the distance d is 0.5 mm (the focus is at the midpoint between blood vessel center and blood vessel wall); 62.92°C when the distance d is 1 mm (the focus is just right at the blood vessel wall); 74.65°C when the distance d is 2.0 mm; and the difference of peak temperature is very small when d is 2.0 mm and 2.5 mm. As the distance d increases ($d \leq 2.0\ mm$), the peak temperature increases, which can be easily explained by the fact that the smaller distance d leads to the larger effect of blood flow cooling. When the distance d is greater than 2.0 mm, there is little effect of blood flow cooling on peak temperature.

Figure 7 demonstrates the thermal lesion region in tissue with different distance between different ultrasonic focus and central axis of blood vessel. When the ultrasonic focus is at the midpoint between the blood vessel center and blood vessel wall (i.e., $d = 0.5\ mm$), there is no thermal lesion region; when the ultrasonic focus is just right at blood vessel wall (i.e., $d = 1\ mm$), the thermal lesion region is an elliptical shape with the size $0.48\ cm \times 0.07\ cm$ excluding the region in the blood vessel; when $d = 1.5\ mm$, the thermal lesion region is an elliptical shape with the size $0.71\ cm \times 0.14\ cm$ excluding the region in the blood vessel; and the thermal lesion region is an elliptical shape with the size $0.75\ cm \times 0.21\ cm$ and $0.75\ cm \times 0.24\ cm$ for $d = 2.0\ mm$ and $d = 2.5\ mm$, respectively. The greater the distance d, the lower the cooling effect of blood flow, and the larger the thermal lesion region, which also has clinical significance. When the tumor is adjacent to a significant blood vessel, the doctor should choose the suitable location of ultrasonic focus, not too close to the vessel wall, especially not in the blood vessel. Otherwise, there is a high probability that the tumor will not be thermal ablated completely.

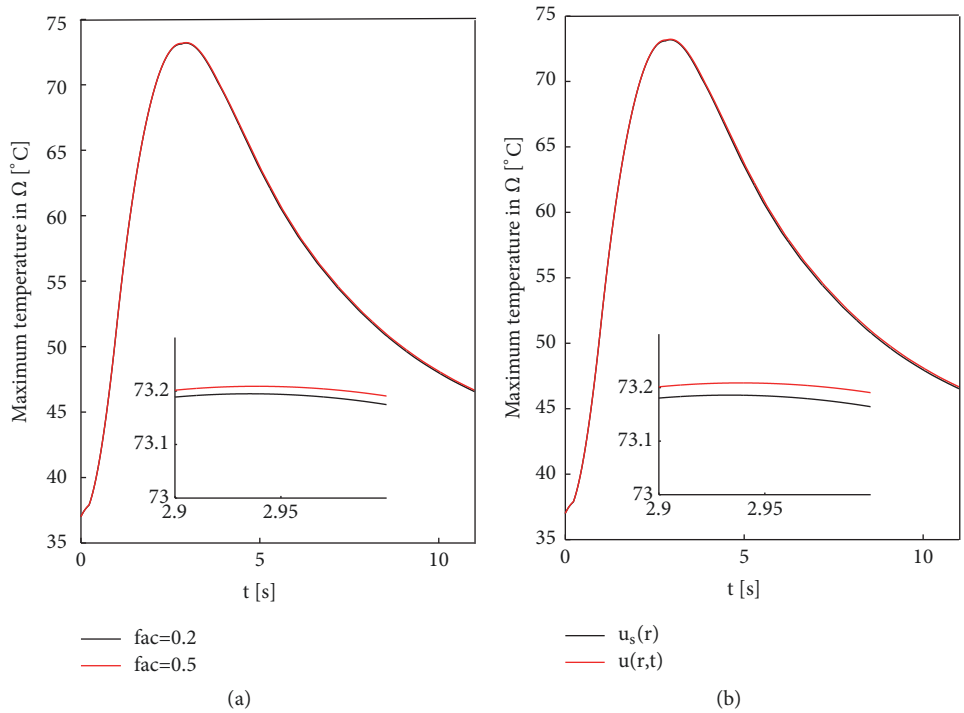

FIGURE 5: Maximum temperature in space $r, z \in \Omega$ versus time: (a) different fac ($fac = 0.2$ and $fac = 0.5$); (b) different blood flow velocity forms (steady parabolic velocity $u_s(r)$ and pulsatile velocity $u(r,t)$). Here, $p_0 = 1.5 \times 10^5\ pa, r_0 = 1\ mm, d = 1.5\ mm, u_{ave} = 5\ cm/s, f_p = 1\ Hz, t_h = 1\ s$.

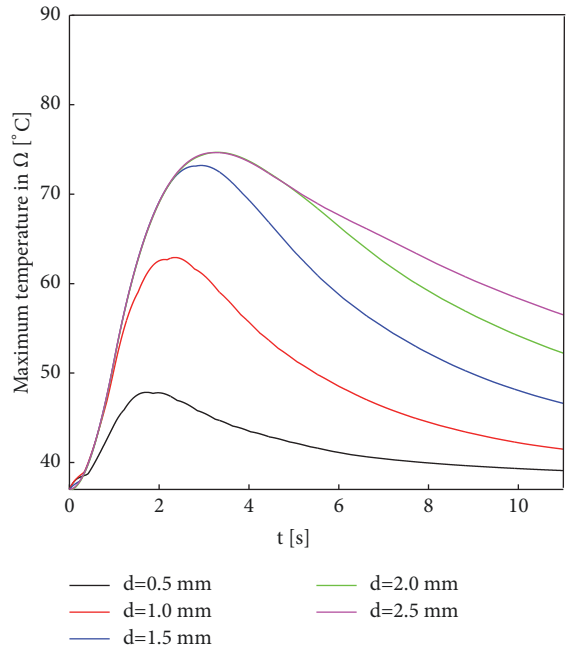

FIGURE 6: Maximum temperature in space $r, z \in \Omega$ versus time with different distance d for $p_0 = 1.5 \times 10^5\ pa, r_0 = 1\ mm, \tau = 1.756\ s, u_{ave} = 5\ cm/s, f_p = 1\ Hz, fac = 0.5, t_h = 1\ s$.

3.4. Blood Vessel Radius. When the ultrasonic focus is right at the center of the blood vessel, the smaller radius gives rise to the greater peak temperature, as shown in Figure 8.

When the blood vessel diameter is less than 0.2 *mm*, there is thermal equilibrium between blood vessel and surrounding tissues, and the effects of the blood vessel on temperature and thermal lesion region can be ignored. In Figure 9, it can be seen that thermal lesion region has only a slight difference between the vascular radius of 0.1 *mm* and without blood vessel and covers the whole blood vessel. When $r_0 = 0.2\ mm$,

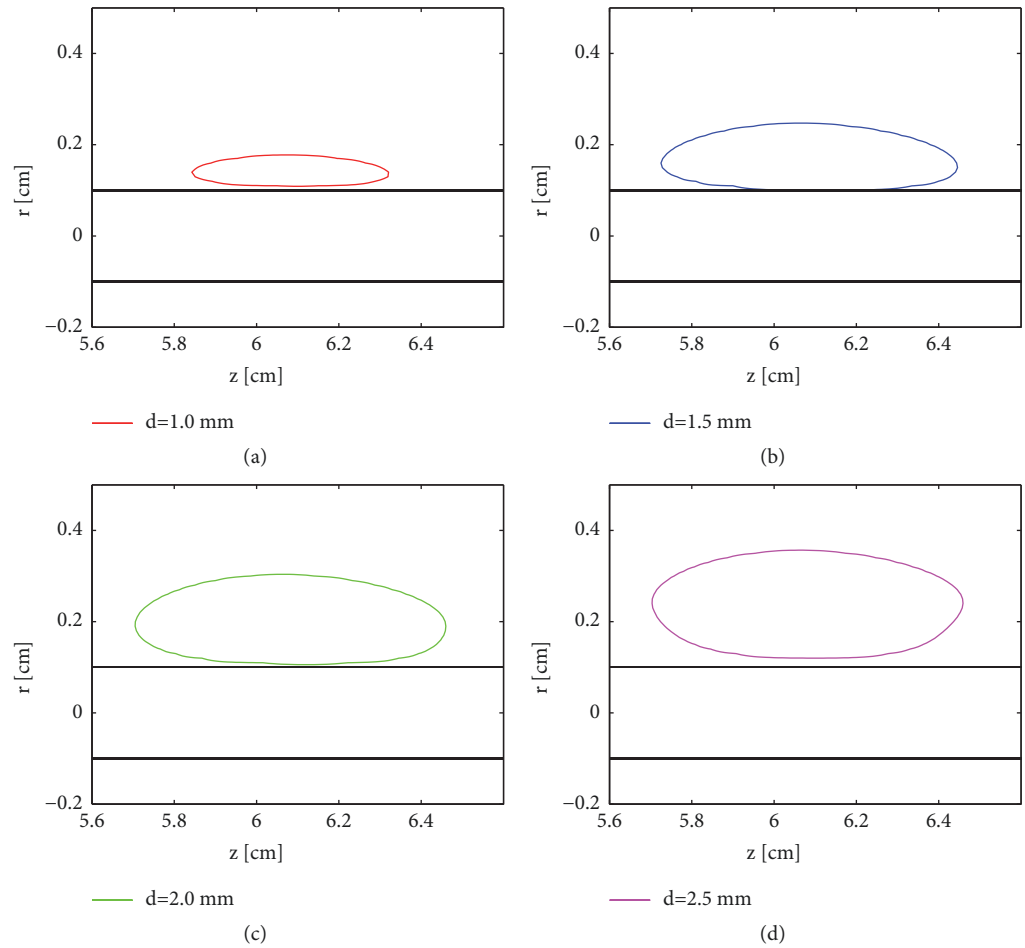

FIGURE 7: Thermal lesion region in space $r, z \in \Omega$ with different distance d for $p_0 = 1.5 \times 10^5\ pa$, $r_0 = 1\ mm$, $\tau = 1.756\ s$, $u_{ave} = 5\ cm/s$, $f_p = 1\ Hz$, $fac = 0.5$, $t_h = 1\ s$.

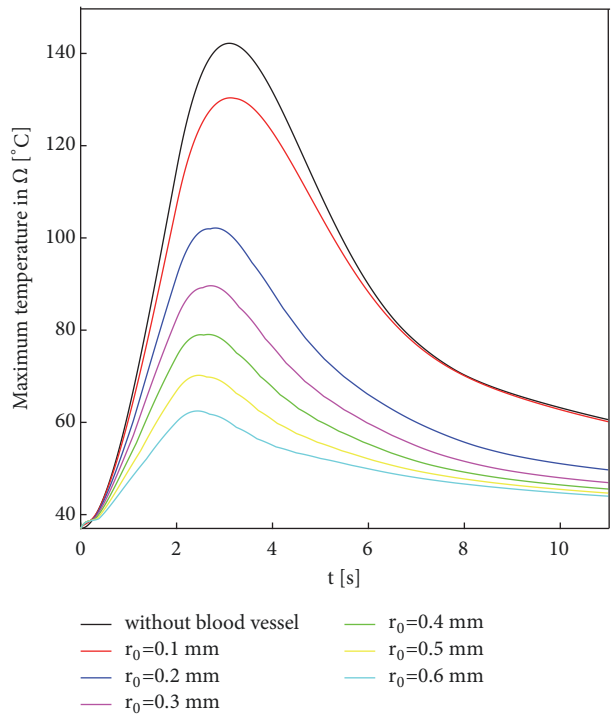

FIGURE 8: Maximum temperature in space $r, z \in \Omega$ versus time with different radius of blood vessel for $p_0 = 2 \times 10^5\ pa$, $u_{ave} = 5\ cm/s$, $d = 0\ mm$, $\tau = 1.756\ s$, $f_p = 1\ Hz$, $fac = 0.5$, $t_h = 2\ s$.

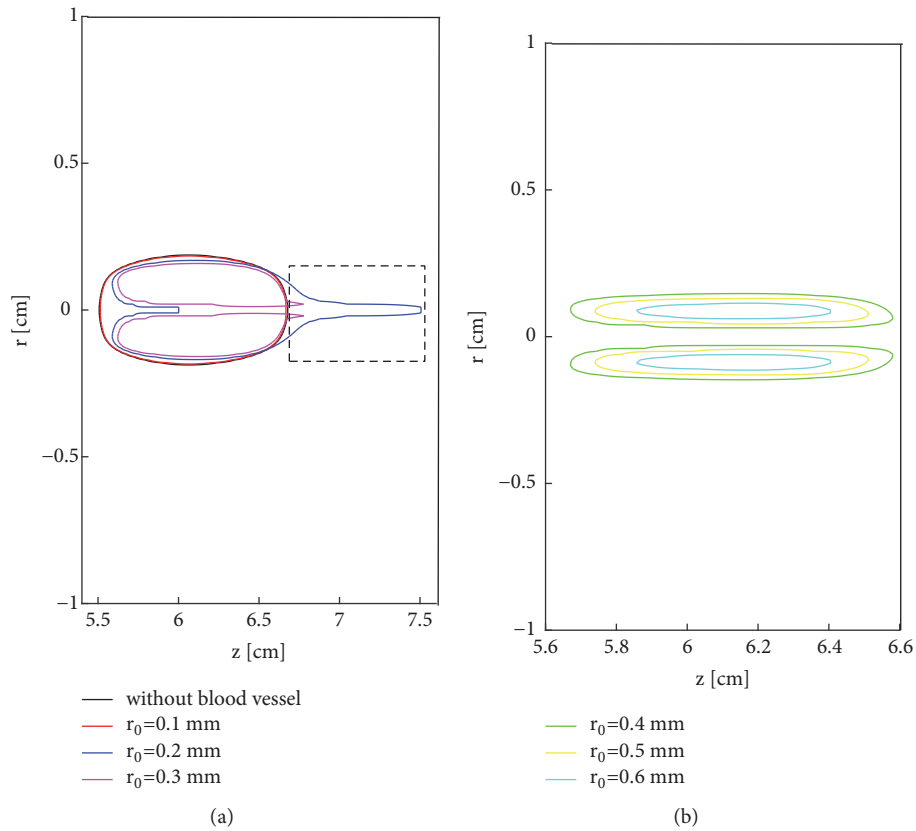

FIGURE 9: Thermal lesion region in space $r, z \in \Omega$ with different radius of blood vessel for $p_0 = 2 \times 10^5\, pa$, $u_{ave} = 5\, cm/s$, $d = 0\, mm$, $\tau = 1.756\, s$, $f_p = 1\, Hz$, $fac = 0.5$, $t_h = 2\, s$.

thermal equilibrium between blood vessel and surrounding tissues is broken. Due to the cooling effect of the blood flow, the thermal doses in some areas of the biological tissue are less than 240 *min* equivalent time at 43°C, resulting in deficit of thermal lesion region. In addition, the part of the thermal lesion region is shaped like tail as shown in the dotted box of Figure 9(a), which may be caused by the comprehensive influence of heat conduction, convective blood cooling, and heat source. It also gives us a hint that HIFU hyperthermia most probably hurts the normal tissue because of the existence of tail-like thermal lesion region. When $r_0 = 0.3\, mm$, it has a greater deficit of thermal region and smaller tail-like thermal lesion region compared with $r_0 = 0.2\, mm$. When the radius of the vessel varies from $0.4\, mm$ to $0.6\, mm$, the thermal lesion region split into two parts. Accordingly, the thermal lesion region with blood vessel radii of 0.2 *mm* and 0.3 *mm* can be considered as a transition stage in the heated tissue with large vessels and without blood vessel. As shown in Figure 9, the smaller blood vessel radius results in the larger thermal region, and the thermal lesion region is very sensitive to the blood vessel radius. Even if the radius of the blood vessel just changes 0.1 *mm*, it also causes very different thermal lesion region.

3.5. Blood Flow Velocity. When the ultrasonic focus is right at the center of the blood vessel, Figure 10 shows the maximum

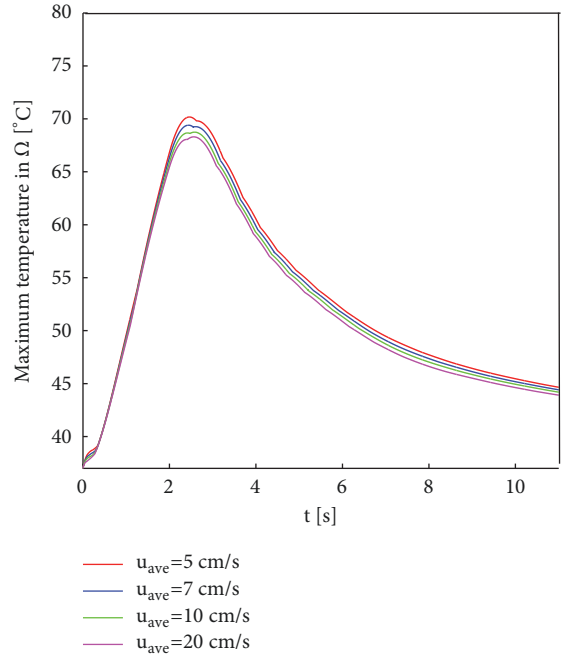

FIGURE 10: Maximum temperature in space $r, z \in \Omega$ versus time with different average velocity of blood flow for $p_0 = 2 \times 10^5\, pa$, $r_0 = 0.5\, mm$, $d = 0\, mm$, $\tau = 1.756\, s$, $f_p = 1\, Hz$, $fac = 0.5$, $t_h = 2\, s$.

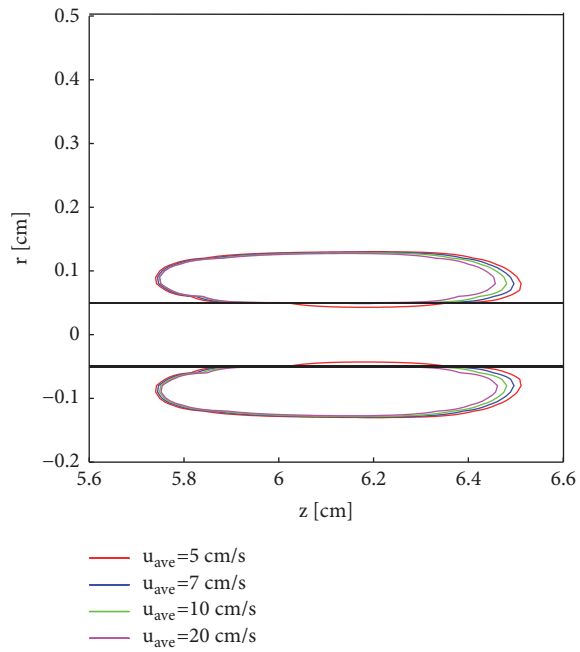

FIGURE 11: Thermal lesion region in space $r, z \in \Omega$ with different average velocity of blood flow for $p_0 = 2 \times 10^5\, pa$, $r_0 = 0.5\, mm$, $d = 0\, mm$, $\tau = 1.756\, s$, $f_p = 1\, Hz$, $fac = 0.5$, $t_h = 2\, s$.

temperature in space $r, z \in \Omega$ versus time with different average velocity of blood flow. The peak temperature is 70.18°C for $u_{ave} = 5\, cm/s$ and 68.30°C for $u_{ave} = 20\, cm/s$ because increasing blood flow velocity causes an increase of cooling effect. When the average blood flow velocity u_{ave} varies from $5\, cm/s$ to $20\, cm/s$, the peak temperature only decreased by 1.88°C, an approximately 2.7% decrease. For different average velocity of blood flow, the thermal lesion region has only a slight difference as shown in Figure 11. In other words, the blood flow velocity has only minor effect on the thermal lesion region.

4. Conclusions

In this paper, TWMBT, improved from the traditional Pennes bioheat transfer model, is employed to study the effects of blood vessel and thermal relaxation time on temperature and thermal lesion region in biological tissue during the HIFU hyperthermia. The heartbeat frequency f_p and amplitude factor fac almost have no effect on temperature and thermal lesion region, and there is almost the same thermal lesion size between steady parabolic velocity and pulsatile velocity. The greater thermal relaxation time leads to smaller thermal lesion region. This phenomenon indicates that TWMBT results in lower temperature and smaller thermal lesion region compared to the classical Pennes bioheat transfer model in the HIFU hyperthermia. The distance between the ultrasonic focus and the central axis of blood vessel also has an important influence on the HIFU hyperthermia treatment. The larger the distance d, the larger the thermal lesion region. The blood vessel radius is very sensitive to the thermal lesion region. When the blood vessel radius r_0 is between $0.2\, mm$ and $0.3\, mm$, it has part of thermal lesion region like a tail, which may hurt the normal tissue. The thermal lesion region is insensitive to blood velocity during the HIFU hyperthermia. All the numerical simulation results are meaningful to guide the doctors to perform HIFU thermal ablation of tumor.

Data Availability

The data used to support the findings of this study are included within the article.

Conflicts of Interest

The authors declare that they have no conflicts of interest.

Acknowledgments

This study is partially supported by the National Nature Science Foundation of China (Nos. 11474090, 11774088, 11174077, and 61502164), Hunan Provincial Natural Science Foundation of China (No. 2016JJ3090), Scientific Research Fund of Hunan Provincial Education Department (No. 16B155), Aid program for Science and Technology Innovative Research Team in Higher Educational Institutions of Hunan Province, Science and Technology Research Program of Chenzhou City (No. CZ2014039), and Research Program of Xiangnan University (No. 2014XJ63).

References

[1] K. Qian, C. Li, Z. Ni, J. Tu, X. Guo, and D. Zhang, "Uniform tissue lesion formation induced by high-intensity focused ultrasound along a spiral pathway," *Ultrasonics*, vol. 77, pp. 38–46, 2017.

[2] S. R. Guntur and M. J. Choi, "Influence of temperature-dependent thermal parameters on temperature elevation of tissue exposed to high-intensity focused ultrasound: Numerical simulation," *Ultrasound in Medicine & Biology*, vol. 41, no. 3, pp. 806–813, 2015.

[3] J. G. Lynn, R. L. Zwemer, A. J. Chick, and A. E. Miller, "A new method for the generation and use of focused ultrasound in experimental biology," *The Journal of General Physiology*, vol. 26, no. 2, pp. 179–193, 1942.

[4] Y. Zhou, "Acoustic power measurement of high-intensity focused ultrasound transducer using a pressure sensor," *Medical Engineering & Physics*, vol. 37, no. 3, pp. 335–340, 2015.

[5] J. Serrone, H. Kocaeli, T. Douglas Mast, M. T. Burgess, and M. Zuccarello, "The potential applications of high-intensity focused ultrasound (HIFU) in vascular neurosurgery," *Journal of Clinical Neuroscience*, vol. 19, no. 2, pp. 214–221, 2012.

[6] S. Qian, T. Kamakura, and M. Akiyama, "Simulation of sound field in a tissue medium generated by a concave spherically annular transducer," *Ultrasonics*, vol. 44, pp. e271–e274, 2006.

[7] J. Hu, S. Qian, and Y. Ding, "Research on adaptive temperature control in sound field induced by self-focused concave spherical transducer," *Ultrasonics*, vol. 50, no. 6, pp. 628–633, 2010.

[8] X. Liu, Y. Zhu, F. Zhang, and X. Gong, "Estimation of temperature elevation generated by ultrasonic irradiation in biological tissues using the thermal wave method," *Chinese Physics B*, vol. 22, no. 2, Article ID 024301, pp. 1–5, 2013.

[9] M. kashcooli, M. R. Salimpour, and E. Shirani, "Heat transfer analysis of skin during thermal therapy using thermal wave equation," *Journal of Thermal Biology*, vol. 64, pp. 7–18, 2017.

[10] C. Cattaneo, "A form of heat conduction equation which eliminates the paradox of instantaneous propagation," *Compte Rendus*, vol. 247, no. 4, pp. 431–433, 1958.

[11] P. Vernotte, "Les paradoxes de la theorie continue de l'equation de la chaleur," *ComptE Rendu*, vol. 246, pp. 3154-3155, 1958.

[12] W. Kaminski, "Hyperbolic heat conduction equation for materials with a nonhomogeneous inner structure," *Journal of Heat Transfer*, vol. 112, no. 3, pp. 555–560, 1990.

[13] K. Mitra, S. Kumar, A. Vedavarz, and M. K. Moallemi, "Experimental evidence of hyperbolic heat conduction in processed meat," *Journal of Heat Transfer*, vol. 117, no. 3, pp. 568–573, 1995.

[14] W. Roetzel, N. Putra, and S. K. Das, "Experiment and analysis for non-Fourier conduction in materials with non-homogeneous inner structure," *International Journal of Thermal Sciences*, vol. 42, no. 6, pp. 541–552, 2003.

[15] Y. Zhang, "Generalized dual-phase lag bioheat equations based on nonequilibrium heat transfer in living biological tissues," *International Journal of Heat and Mass Transfer*, vol. 52, no. 21-22, pp. 4829–4834, 2009.

[16] W. Dai, H. Wang, P. M. Jordan, R. E. Mickens, and A. Bejan, "A mathematical model for skin burn injury induced by radiation heating," *International Journal of Heat and Mass Transfer*, vol. 51, no. 23-24, pp. 5497–5510, 2008.

[17] M. Jaunich, S. Raje, K. Kim, K. Mitra, and Z. Guo, "Bio-heat transfer analysis during short pulse laser irradiation of tissues," *International Journal of Heat and Mass Transfer*, vol. 51, no. 23-24, pp. 5511–5521, 2008.

[18] F. Jiang, M. He, Y. J. Liu, Z. B. Wang, L. Zhang, and J. Bai, "High intensity focused ultrasound ablation of goat liver in vivo: Pathologic changes of portal vein and the "heat-sink" effect," *Ultrasonics*, vol. 53, no. 1, pp. 77–83, 2013.

[19] H. H. Pennes, "Analysis of tissue and arterial blood temperatures in the resting human forearm," *Journal of Applied Physiology*, vol. 1, no. 2, pp. 93–122, 1948.

[20] M. C. Kolios, M. D. Sherar, and J. W. Hunt, "Blood flow cooling and ultrasonic lesion formation," *Medical Physics*, vol. 23, no. 7, pp. 1287–1298, 1996.

[21] P. Hariharan, M. R. Myers, and R. K. Banerjee, "HIFU procedures at moderate intensities - Effect of large blood vessels," *Physics in Medicine and Biology*, vol. 52, no. 12, article no. 011, pp. 3493–3513, 2007.

[22] M. A. Solovchuk, T. W. H. Sheu, W.-L. Lin, I. Kuo, and M. Thiriet, "Simulation study on acoustic streaming and convective cooling in blood vessels during a high-intensity focused ultrasound thermal ablation," *International Journal of Heat and Mass Transfer*, vol. 55, no. 4, pp. 1261–1270, 2012.

[23] A. A. Doinikov, A. Novell, P. Calmon, and A. Bouakaz, "Simulations and measurements of 3-D ultrasonic fields radiated by phased-array transducers using the westervelt equation," *IEEE Transactions on Ultrasonics, Ferroelectrics and Frequency Control*, vol. 61, no. 9, pp. 1470–1477, 2014.

[24] F. A. Duck, *physical property of tissues a comprehensive reference book*, Harcourt Brace Jovanovich, London, uk, 1990.

[25] J. Huang, R. G. Holt, R. O. Cleveland, and R. A. Roy, "Experimental validation of a tractable numerical model for focused ultrasound heating in flow-through tissue phantoms," *The Journal of the Acoustical Society of America*, vol. 116, no. 4 I, pp. 2451–2458, 2004.

[26] J. Liu, X. Chen, and L. X. Xu, "New thermal wave aspects on bum evaluation of skin subjected to instantaneous heating," *IEEE Transactions on Biomedical Engineering*, vol. 46, no. 4, pp. 420–428, 1999.

[27] T.-C. Shih, T.-L. Horng, H.-W. Huang et al., "Numerical analysis of coupled effects of pulsatile blood flow and thermal relaxation time during thermal therapy," *International Journal of Heat and Mass Transfer*, vol. 55, no. 13-14, pp. 3763–3773, 2012.

[28] Y. Huo and G. S. Kassab, "Pulsatile blood flow in the entire coronary arterial tree: Theory and experiment," *American Journal of Physiology-Heart and Circulatory Physiology*, vol. 291, no. 3, pp. H1074–H1087, 2006.

[29] S. A. Sapareto and W. C. Dewey, "Thermal dose determination in cancer therapy," *International Journal of Radiation Oncology, Biology & Physics*, vol. 10, no. 6, pp. 787–800, 1984.

[30] C. Damianou and K. Hynynen, "Focal spacing and near-field heating during pulsed high temperature ultrasound therapy," *Ultrasound in Medicine & Biology*, vol. 19, no. 9, pp. 777–787, 1993.

[31] I. M. Hallaj and R. O. Cleveland, "FDTD simulation of finite-amplitude pressure and temperature fields for biomedical ultrasound," *The Journal of the Acoustical Society of America*, vol. 105, no. 5, pp. L7–L12, 1999.